Pergamon

Journal of Atmospheric and Terrestrial Physics, Vol. 57, No. 5, pp. 575–585, 1995

0021-9169/95 $9.50+0.00

0021-9169(94)00082-4

An experimental investigation of atmospheric electricity and lightning activity to be performed during the descent of the Huygens Probe onto Titan

R. Grard,* H. Svedhem,* V. Brown,† P. Falkner‡ and M. Hamelin§

* Space Science Department of ESA, ESTEC, P.O. Box 299, 2200 AG Noordwijk, The Netherlands
† Instituto de Astrofisica de Andalucia, C.S.I.C., Apartado Postale 2144, 18080 Granada, Spain
‡ Space Research Institute, Austrian Academy of Sciences, Inffeldgasse 12, 8010 Graz, Austria
§ Laboratoire de Physique et Chimie de l'Environnement, CNRS, 3A Avenue de la Recherche Scientifique, 45071 Orléans Cédex, France

(*Received in final form* 19 *May* 1994; *accepted* 27 *June* 1994)

Abstract—No terrestrial-like electrical activity was observed during the Voyager 1 flyby of Titan on 12 November 1980, in spite of a predicted global lightning energy dissipation rate of 4×10^{-6} Wm^{-2}. This lack of evidence does not, however, rule out the existence of electrical discharges with magnitudes, rates of occurrence and spectral characteristics drastically different from those known on Earth, owing to large dissimilarities between the temperatures, chemical compositions and, especially, electrical conductivities of the two atmospheres. Towards the end of the year 2004, the ESA probe Huygens will be jettisoned from the NASA Saturn orbiter, Cassini. This probe will descend onto Titan and perform *in situ* measurements during a period of 3 h, from an altitude of 170 km down to the satellite surface where the atmospheric pressure reaches 1.6×10^5 Pa. The Huygens scientific payload will include a set of instruments entirely dedicated to the detection of lightning and to the characterization of the electrical properties of the atmosphere and surface. An electric antenna will search for natural emissions in the frequency range 0–10 kHz, at altitudes lower than those of ionized layers opaque to electromagnetic waves, and measure the magnitude of static electric fields due to charge separation. The conductivity of the atmosphere and the existence of free electrons will be checked during the whole descent with a combination of quadrupolar and relaxation probes; a microphone will also record acoustic phenomena associated with electrical discharges and atmospheric processes. The impedance of the surface will be evaluated from the measurements collected with a radar during the descent and a quadrupolar array after touch down.

1. INTRODUCTION

The possible occurrence of electrical discharges in the atmosphere of Titan, the largest satellite of the planet Saturn, has potential consequences for the production of trace gaseous constituents, the formation of aerosols and the accumulation of soot deposits over the surface (Borucki *et al.*, 1984). The study of these phenomena is also important because it leads to a better understanding of similar processes which take place in our own atmosphere.

We first recapitulate briefly the principal features of the Huygens Probe, which will explore the atmosphere of Titan in 2004. We describe the model electrical environment of the satellite and a thunderstorm model directly scaled from that applicable to the Earth. We then estimate the number of lightnings which can be possibly observed during the descent of the Probe.

The function and configuration of the Permittivity, Wave and Altimetry (PWA) analyser are presented, and its capability to identify electrical activity in the atmosphere of Titan is assessed.

2. AN EXPLORATION OF TITAN'S ATMOSPHERE

2.1. *The Huygens mission*

The Cassini mission will carry out an investigation of the Saturnian system. The spacecraft will be launched in October 1997 and will consist of a Saturn Orbiter developed by NASA and a Titan probe, Huygens, supplied by ESA (Matson, 1992; Lebreton, 1992). Huygens will be separated from the Orbiter upon arrival in the vicinity of Titan, which orbits around Saturn at a distance of 20 planetary radii, and enter the atmosphere of this satellite 22 days later, on 17 November 2004.

Possible descent profiles of the probe are illustrated in Fig. 1, following the release of the heat shield and the deployment of the first parachute. Most scientific instruments will be operated from an altitude of about

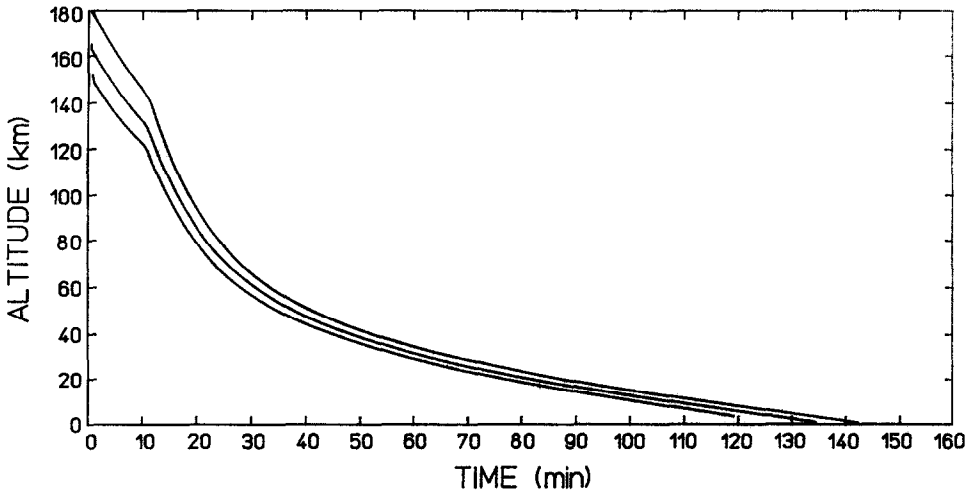

Fig. 1. Typical altitude vs. time profiles of the Huygens Probe during its descent in the atmosphere of Titan.

170 km for a period of 2–3 h which will come to an end a few minutes after surface touch-down.

The scientific payload consists of six instruments, namely:

— gas chromatograph and mass spectrometer;
— aerosol collector and pyrolyser;
— descent imager/spectral radiometer;
— surface science package;
— Doppler wind experiment; and
— atmosphere structure instrument.

The Permittivity, Wave and Altimetry analyser, which is an integral part of HASI, the Huygens Atmospheric Structure Instrument (Fulchignoni *et al.*, 1990), is primarily dedicated to the study of atmospheric electricity. Searching for lightning activity in the atmosphere of Titan is one of the scientific objectives of the PWA analyser.

2.2. *A search for atmospheric electricity*

Our quest for information about potential electrical activity in the atmosphere of Titan is partly stimulated by the mere fact that this phenomenon is known to take place on several planets. Furthermore, many space investigations assume experimental approaches which are often suggested to us by the nature of the physical processes which take place in our own environment.

The global electric diagram of the terrestrial atmospheric circuit is represented in Fig. 2 (Fleagle and Businger, 1963); it illustrates a number of features which bear evidence of a thunderstorm activity, namely:

— electric discharges;
— atmospheric currents;
— electric potential gradients;
— ionospheric conductivity; and
— surface electric properties.

Some of these phenomena are not directly observable; the existence of an atmospheric current, for example, can only be inferred from measurements of the atmospheric conductivity and potential gradient.

Individual electric discharges, on the other hand, can be detected directly with optical instruments (flashes), radio receivers (sferics) or microphones (thunderclaps). Furthermore, Extremely Low Frequency (ELF) electromagnetic radiation gives rise to the Schumann resonances in the spherical waveguide formed by the surface of the body and the inner boundary of the ionosphere. The spectrum of the signal observed on Earth is shown in Fig. 3 (Polk, 1982); the resonance frequencies are inversely proportional to the radius of the body and should therefore be 2.5 times larger in the case of Titan.

3. MODEL ELECTRICAL ENVIRONMENT

3.1. *Ionospheric profile and sferics propagation*

The electron density profile shown in Fig. 4 was obtained by merging (1) an upper layer induced by solar photon and magnetosphere electron impacts, predicted by Ip (1990), (2) a lower layer associated with galactic cosmic ray ionization, with and without the presence of aerosols, proposed by Borucki *et al.*

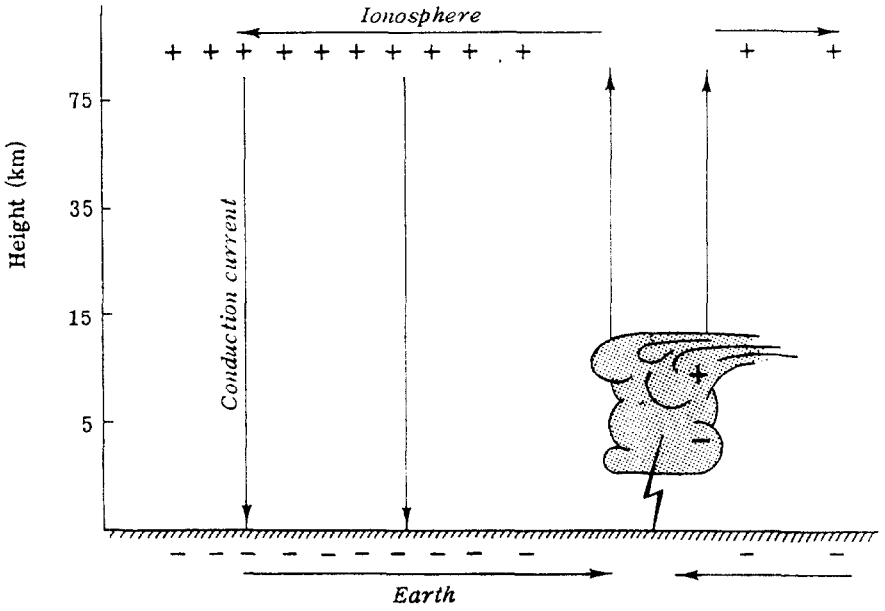

Fig. 2. Schematic representation of the separation of charges by thunderstorms and the global circulation of associated electric currents in the atmosphere of the Earth (Fleagle and Businger, 1963).

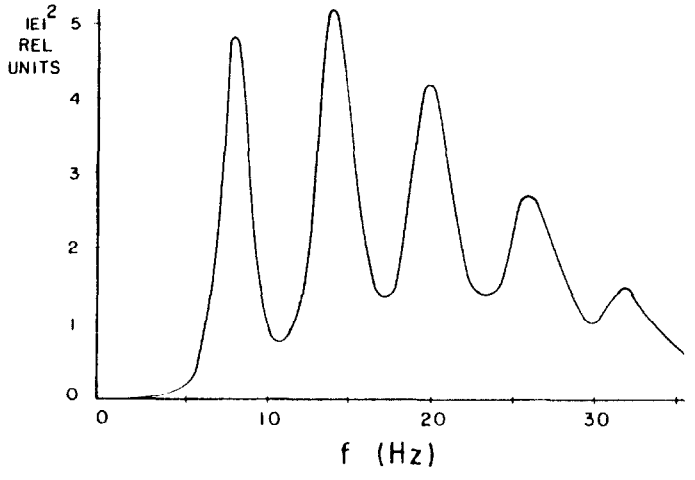

Fig. 3. Energy spectrum of the electromagnetic waves generated by lightning activity in the Earth ionosphere cavity showing peaks at the Schuhmann resonance frequencies (Polk, 1982).

(1987), and (3) an intermediate layer due to meteoric impact (Grard, 1992).

The Voyager 1 occultation measurements have set an upper limit of 3.5×10^5 cm^{-3} for the electron density (Lindal *et al.*, 1983) and the meteoric layer must therefore be considered, at most, as a sporadic feature.

Figure 5 is a diagram which shows the altitude ranges where the propagation of an electromagnetic wave of a given frequency is either practically imperturbed, severely damped or merely impossible (hatched area). The plasma angular frequency, ω_p, is derived from Fig. 4, and the estimation of the electron plasma frequency is based on the atmospheric model of Lellouch and Hunten (1987). Such a diagram indicates that waves with frequencies less than a few hundred kHz are trapped within the ionospheric cavity and are more easily observed with an atmospheric probe than from an orbiter.

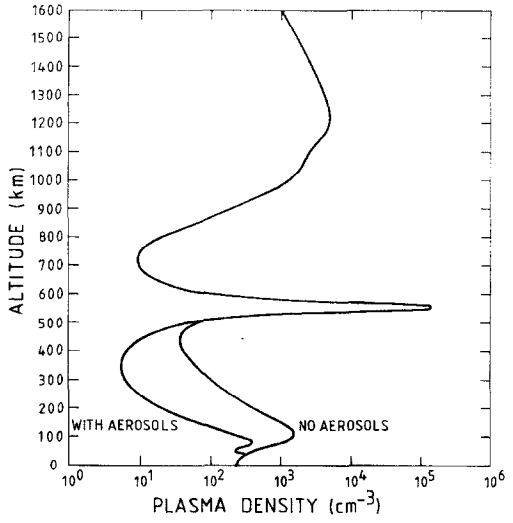

Fig. 4. Vertical profile of the electron density in Titan's atmosphere, merging a meteoric layer, at an altitude of 500 km (Grard, 1992), with an upper layer induced by solar photon and magnetospheric electron impacts (Ip, 1990) and a lower layer due to galactic cosmic rays, with and without aerosols (Borucki *et al.*, 1987).

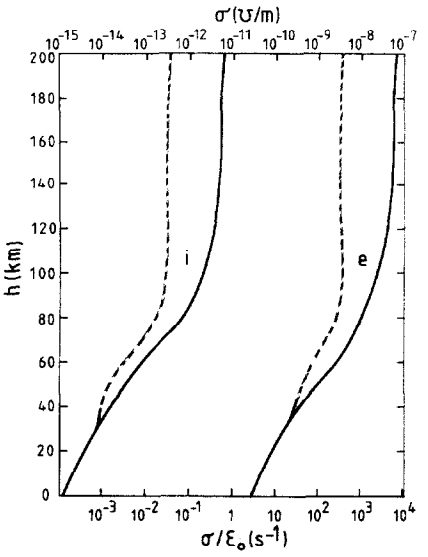

Fig. 6. Models of the ion (i) and electron (e) conductivity profiles, with and without aerosols (dash and full lines, respectively).

3.2. *Atmospheric conductivity*

The plasma density model of Borucki *et al.* (1987), which corresponds with the lower part of the profile shown in Fig. 4, and the pressure and neutral density models of Lellouch and Hunten (1987) are combined to give the atmospheric conductivity, σ, and inverse time constant, σ/ε_0, where ε_0 is the permittivity of free space. The conductivity profiles for ions (i) and electrons (e) are plotted in Fig. 6; the two branches of each profile correspond, as in Fig. 4, to the presence or absence of aerosols.

The electron conductivity is very large in the atmosphere of Titan, relative to the situation encountered on Earth, owing to the fact that nitrogen and other

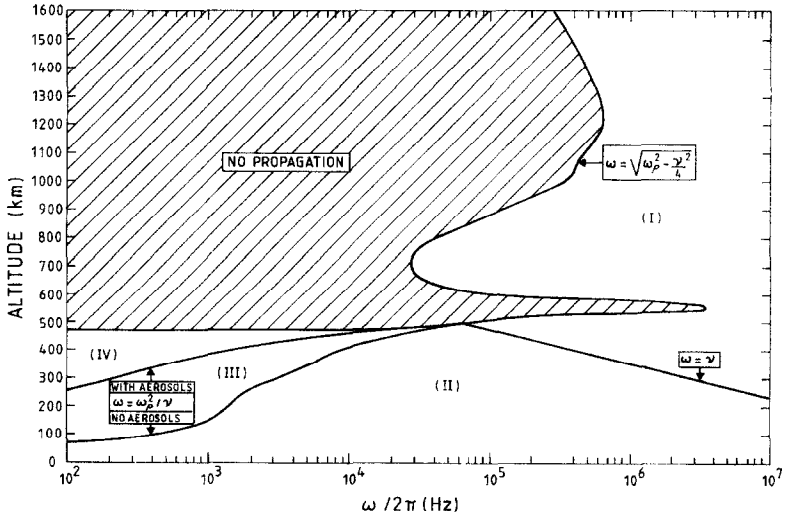

Fig. 5. Diagram illustrating the regions where the propagation of electromagnetic waves is either impossible (hatched area), practically unperturbed (areas I and II), or severely dampened (area IV). Area III is part of area II or IV, when aerosols are present or absent, respectively.

atmospheric constituents on Titan do not form any negative ions (Borucki *et al.*, 1987).

4. POSSIBLE LIGHTNING ACTIVITY ON TITAN

4.1. *Basic equations*

If we assume that Earth-like atmospheric processes also take place on Titan (Borucki *et al.*, 1984), the power density available for lightning can be written:

$$P = \tfrac{1}{4} SFR. \tag{1}$$

The solar flux, S, equals 16 Wm^{-2} at the mean solar distance of Saturn, 9.54 AU, but the fraction of solar energy actually converted into convective motion, F, is estimated to be of the order of only 10^{-2} (McKay *et al.*, 1991). The ratio of lightning to convection power densities, R, is assumed to lie between the experimental values derived for Earth and Jupiter and is taken equal to 4×10^{-6}, with an uncertainty of one order of magnitude (Borucki *et al.*, 1984). The factor 1/4 merely shows that only the cross-section of the satellite is illuminated by the Sun, whereas lightning activity may take place anywhere over the surface of Titan.

Replacing these numerical values in equation (1) yields a lightning energy dissipation rate of 1.6×10^{-7} Wm^{-2}, a figure previously quoted by Lorenz (private communication), which must also equal the product of the flash rate per unit area, n, by the average energy dissipated during each event, W:

$$P = n\,W. \tag{2}$$

Assuming that all lightnings are identical and evenly distributed over the surface of the satellite, the number of events recorded during the descent of the probe takes the form:

$$N = \int_0^T n\,A\,dt, \tag{3}$$

where T is the duration of the descent, about 3 h, and A is the area covered by the PWA receiver as a function of time t. If, in addition, the lightnings are also evenly distributed in time, equations (2) and (3) can then be combined to yield

$$N = \frac{P}{W} \int_0^t A\,dt, \tag{4}$$

or

$$N = A_0\,T\,P/W, \tag{5}$$

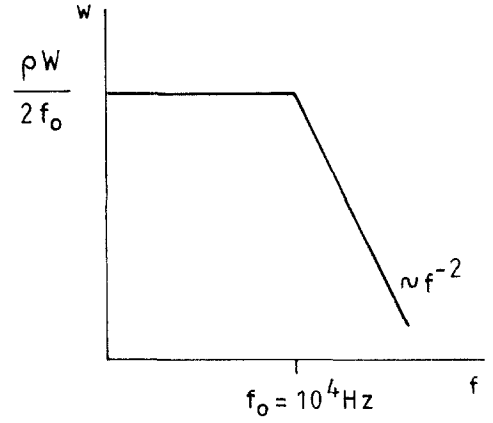

Fig. 7. Energy distribution model for terrestrial lightning.

where A_0 is the average area covered by the receiver during the probe descent.

If diffraction and ionospheric reflection are ignored and if the receiver characteristics and the frequency spectrum of the sferics are given, the detection of any event depends only upon the geometric visibility and the distance of the electromagnetic source.

The relation between the nominal sensitivity, E_0 ($Vm^{-1}Hz^{-1/2}$), and integration time, Δt (s), of the receiver and the spectral energy density threshold, U_0 ($Jm^{-2}Hz^{-1}$)), of any detectable impulsive electromagnetic signal with duration much less than Δt is simply

$$E_0^2 \Delta t = Z_0\,U_0, \tag{6}$$

where $Z_0 = 120\pi\ \Omega$ is the impedance of free space.

If the ground is a perfect conductor and the radiation is isotropic, the corresponding spectral energy is given by

$$w = 2\pi d^2\,U_0, \tag{7}$$

where the distance d characterizes the range of the receiver and

$$\int_0^\infty w\,df = \rho W; \tag{8}$$

the fraction of the flash energy radiated as electromagnetic waves, ρ, is of the order of 5×10^{-5} (Desch and Kaiser, 1990).

We assume, as a working hypothesis that, as on the Earth (Uman, 1987; Lanzerotti *et al.*, 1989), the spectrum of the radiated energy is approximately constant at low frequencies and falls off as f^{-2} above $f_0 = 10$ kHz (Fig. 7). It comes from equation (7), that

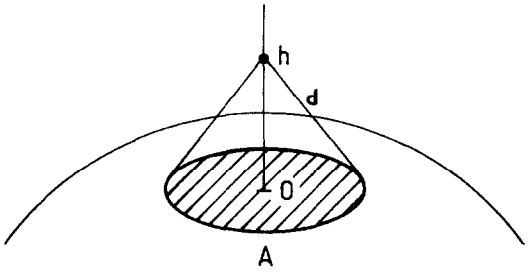

Fig. 8. Surface covered by the receiver at an altitude h above the surface of Titan.

$$w = \frac{\rho W}{2f_0} \tag{9}$$

in the frequency domain covered by the receiver, $f \ll f_0$. Combining equations (6), (7) and (9) yields the range distance

$$d = \left(\frac{Z_0}{4\pi}\frac{\rho W}{f_0}\frac{1}{E_0^2 \Delta t}\right)^{1/2}. \tag{10}$$

Assuming, for simplicity, that lightnings occur at very low altitudes, the surface covered by the receiver is the spherical cap defined by the contact between a sphere and a cone (Fig. 8). The sphere has the radius of Titan, $R_T = 2575$ km; the apex of the cone lies at an altitude h and the length of the generating line is given by equation (10). The situation illustrated in Fig. 7 corresponds with the condition $h < d < d_H$, where

$$d_H \simeq (2hR_T)^{1/2} \tag{11}$$

is the distance between the receiver and the horizon. The area A equals 0 when $d < h$ and is close to $2\pi hR_T$ when $d \geqslant d_H$, since $h \ll R_T$.

4.2. *Estimated lightning production*

An estimation of the number of events possibly recorded during the descent, N, is given in Fig. 9 as a function of average flash energy, in the case where $\Delta t = 25$ ms and $E_0 = 1.4\ \mu\text{Vm}^{-1}\text{Hz}^{-1/2}$ and under the assumption that the probe vertical velocity is constant. The upper horizontal axis gives the range d associated with a given flash energy W (equation (10)); $H = 170$ km is the altitude of the probe at the beginning of the descent and $(2\ HR_T)^{1/2} = 936$ km is the distance of the horizon seen from this altitude. An upper limit to the total number of detectable flashes

$$N_0 = \frac{Z_0}{4}\frac{\rho P}{f_0}\frac{T}{E_0^2 \Delta t}, \tag{12}$$

is derived by replacing

$$A_0 = \pi d^2 \tag{13}$$

in equation (5), which is equivalent to assuming that the receiver is located on a flat surface or, in other words, that $h = 0$ and $R_T = \infty$.

The number of events can also be given in analytical form, for low and high flash energies. When $d < H$, sferics can only be detected when the probe altitude is less than d, which gives

$$A_0 = \frac{2\pi d^3}{3H} \tag{14}$$

and

$$N = \frac{2N_0^{3/2}}{3H}\left(\frac{W}{\pi PT}\right)^{1/2}. \tag{15}$$

When $d > (2HR_T)^{1/2}$, flashes occurring beyond the horizon cannot propagate to the receiver since we ignore any possible reflection from the ionosphere; we then obtain

$$A_0 = \pi HR_T \tag{16}$$

and

$$N = \pi HR_T PT/W. \tag{17}$$

Parenthetically, the average area of the surface bounded by the horizon during the descent (equation (16)) is only 1.72% that of the satellite. However, if Titan were scaled up to the size of the Earth, this area would be comparable with that of the United States.

In fact, (1) the vertical velocity of the probe is not constant and is lower in the terminal phase of the descent (Fig. 1); (2) the lightning activity does not take place on the surface but, more likely, in the altitude range 0–35 km (Borucki *et al.*, 1984); (3) diffraction and wave trapping in the ionospheric cavity extend the range of the receiver well beyond the horizon; and (4) this is assuming that a typical flash energy does not imply that all events are identical. All these considerations probably entail a significant increase and flattening of the curve representing the integrated count number vs. average flash energy.

The results of Voyager 1 exclude, in principle, the existence of lightnings with energies larger than $W_0 = 10^6$J, as indicated by the hatching in Fig. 9 (Desch and Kaiser, 1990), but this prediction is based on the assumption that the power spectrum of the sferics has the same characteristics on Titan and on

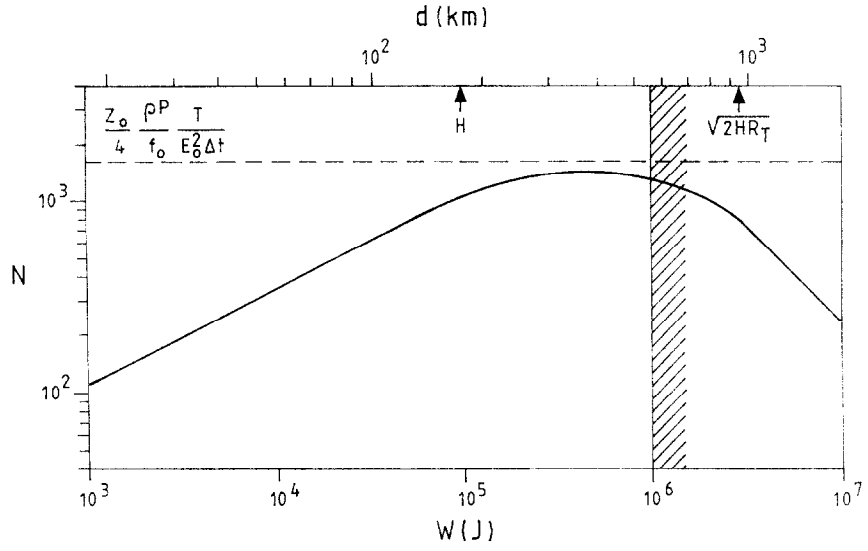

Fig. 9. Total number of sferics, N, recorded during the descent of Huygens as a function of lightning energy, W.

Earth (Fig. 7). If f_0 had been chosen to be equal to 10^3 Hz, for example, on the basis of possible differences in discharge mechanisms, then the upper limits of the flash energy and of the total count number, W_0 and N_0, would have both been increased by one order of magnitude. In fact, the flash rate may be comparable with that at the Earth, but the average energy per flash should be 10^3–10^4 times lower (Desch and Kaiser, 1990).

The nominal flyby distance of Cassini is 1500 km, compared with 4000 km for Voyager 1, which entails an 8.5 dB reduction of the lightning energy threshold W_0 for the former, all other things being equal.

4.3. *Potential hazard for the Huygens Probe*

Estimating the number of discharges with a given energy which might occur in the close vicinity of the probe, say within a distance r_c, quantifies the potential hazard associated with atmospheric electricity.

The number of these events is written

$$N = \pi r_c^2 n T_c \tag{18}$$

where $T_c \simeq 5000$ s is the time spent by the probe below 35 km (Fig. 1), at altitudes where electric discharges are likely to occur, and n is the flash rate defined by equation (2). This relation can be rewritten

$$r_c = \sqrt{\frac{N_c W}{\pi P T_c}}, \tag{19}$$

or

$$r_c(m) = 20\sqrt{N_c W(J)}, \tag{20}$$

from which one estimates, for example, that there is only one chance in 100, $N_c = 10^{-2}$, to detect a flash of 10^6J within a radius of 2 km around the probe.

5. THE PWA ANALYSER

5.1. *Functions*

The simplified block diagram shown in Fig. 10 illustrates most of the functions of the Permittivity, Wave and Altimetry analyser. Natural signals are detected with an electric antenna made of two sensors, RX1 and RX2, connected to preamplifiers through coupling capacitors, partly to minimize the risk of saturation due to triboelectric effects; its effective length is of the order of 2 m.

In the active mode, a sinusoidal current generated with a synthesizer and a digital-to-analogue converter (DAC) is injected in the medium with another dipole, TX1 and TX2, while the received voltage is simultaneously measured with the first dipole. The ratio of the received voltage to emitted current, i.e. the mutual impedance of the quadrupole, yields the conductivity of the atmosphere (Storey *et al.*, 1969). The same instrument also measures the complex permittivity of the surface, liquid or solid, and its ability to conduct electric currents (Grard, 1990a, b). The atmospheric conductivity is independently measured with two relaxation probes, RLX1 and RLX2. These sensors are momentarily polarized with a voltage gen-

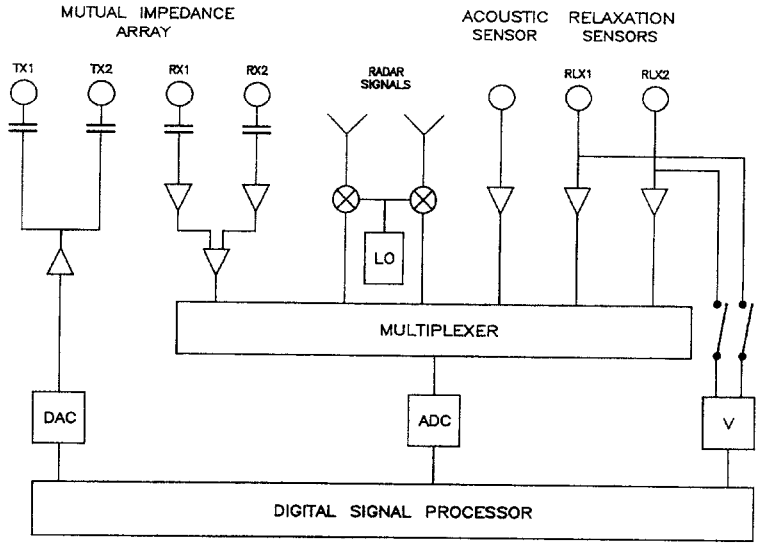

Fig. 10. Block diagram of the PWA analyser.

erator (V) at potentials of ± 5 V; the time constants of the subsequent decays of potential yield the electron and ion conductivities of the medium.

In the passive mode, that is when the voltage generator is disconnected, these probes form two independent monopoles and can measure the quasi-static electric fields which drive the atmospheric currents.

The low frequency measurements of the surface permittivity performed with the quadrupolar probe will be compared with the information collected with the radar altimeters at frequencies of 15.4 and 15.8 GHz. The outputs of these facility instruments result from the beating of the FMCW transmitted signals with the received signals and are made available to HASI for analysis. The intermediate frequency signals, at around 200 kHz, are mixed with that of a local oscillator (LO), and transposed into the frequency bandwidth of the analyser, 0–15 kHz. The strength of the received signal is a function of several parameters; one of those is the reflection coefficient which, in the case of normal incidence, is written:

$$R = |(1-\sqrt{\varepsilon_r})/(1+\sqrt{\varepsilon_r})|, \qquad (21)$$

where ε_r is the relative complex permittivity of the surface. A microphone completes the set of sensors; this acoustic sensor will search for possible thunderclaps and also noise generated by liquid drops or solid particles impacting the surface of the Huygens Probe.

The signals delivered by the electric antenna, the radar altimeter, the acoustic sensor and the relaxation probes are fed into a digital signal processor (ADSP 2100) through a multiplexer and an analogue-to-digital converter (ADC).

The nominal sensitivities, dynamic ranges and frequency ranges of the detectors are listed in Table 1. The time and frequency resolutions of the measurements are controlled with the signal processor, but they are inherently limited by the capability of the onboard software and the rate of the telemetry allocated to PWA, about 800 bits/s on average during the whole descent. Assuming that the model described in section 4 is valid and putting $\Delta t = 25$ ms in equations (12), (15) and (17), for example, yields $N_0 = 1628$ as an upper limit to the number of detectable flashes at mid energies, $N = 3.5\sqrt{W(\mathrm{J})}$ in the lower range, and $N = 2.4 \times 10^9/W(\mathrm{J})$ in the upper range. The maximum number of observable events can, of course, not be increased to any arbitrary level since Δt must remain much larger than f_0^{-1}.

5.2. *Accommodation*

The accommodation of the instrument is illustrated in Fig. 11. The electric sensors are mounted on two articulated booms, shown in stowed and deployed configurations; the booms are fixed on the outer ring of the probe at diametrically opposed locations. The acoustic sensor is attached at the base of a stub which carries the pressure and temperature sensors of HASI. Figure 11 also shows the instrument platform with the two preamplifier units which condition the signals delivered by the receiver and relaxation sensors and the main HASI electronic box which contains the

Table 1. The measuring capability of the PWA analyser

Measurement	Threshold	Dynamic range	Frequency range
AC electric fields	$1.4\ \mu Vm^{-1}Hz^{-1/2}$	80 dB	≃0–10 kHz
DC electric fields	$40\ mVm^{-1}$	50 dB	0–100 Hz
Acoustic noise	10 mPa	83 dB	0 Hz–6 kHz
Measurement	**Range**		**Time resolution**
Ion conductivity	10^{-15}–$10^{-11}\ \Omega m^{-1}$		1 min
Electron conductivity	$>10^{-11}\ \Omega m^{-1}$		1 s

remaining analogue circuitry and the digital signal processor of the PWA analyser.

6. CONCLUSION

The PWA analyser will perform direct observations of DC and AC electric fields and measure the ion and electron conductivities in the atmosphere. The ground impedance will be estimated in two ways, using a quadrupolar array at low frequencies and a radar technique at high frequencies. The volume density of the atmospheric charged particles will be subsequently derived by merging the ion and electron conductivity data with the information collected during the descent by the pressure and temperature sensors, which are also part of HASI. Ion and electron densities are largely controlled by recombination on aerosols; conductivity measurements will therefore provide information about the distribution of aerosols as a function of altitude (Borucki and Fulchignoni, 1992).

It is anticipated that this global set of measurements, corroborated by the results obtained with other

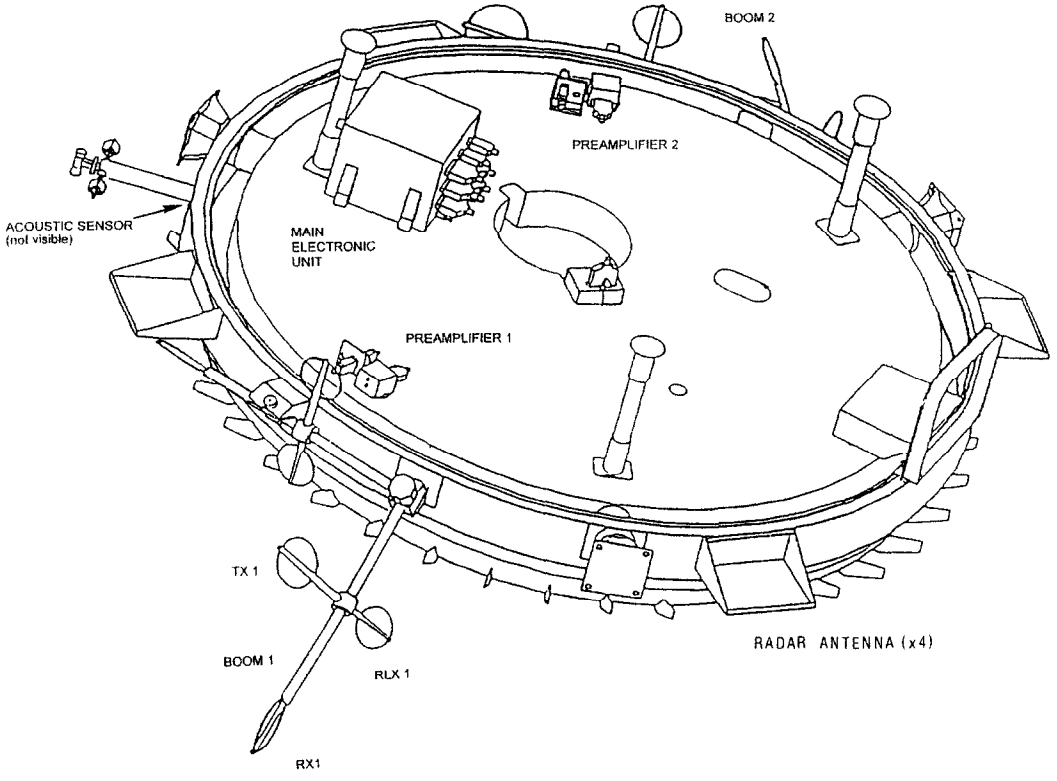

Fig. 11. Accommodation of the HASI instrument, PWA analyser and radar antennas on the payload platform (cabling and other instruments or subsystems not shown).

instruments carried both by the Huygens Probe (Imager/Spectral Radiometer, Surface Science Package) and the Cassini Orbiter (Imager, Spectrometer and Wave Receiver), will either confirm or deny that the atmospheric electricity models developed for the Earth can be extrapolated to Titan. These observations will tell us whether a simple scaling can reconcile the apparent diversity of the two environments or whether drastically different physical processes are at work in the atmospheres of the Earth and Titan.

Acknowledgements—The authors wish to thank Ralph Lorenz for useful discussions and valuable comments. This research has been partially supported by the Spanish Comisión Interministerial de Ciencia y Technologica under contract ESP 93-0338.

REFERENCES

Borucki W. J., Levin Z., Whitten R. C., Keezee R. G., Capone L. A., Summers A. L., Ton O. B. and Dubach J. 1987 Predictions of the electrical conductivity and charging of the aerosols in Titan's atmosphere. *Icarus* **72,** 604–622.

Borucki W. J. and Fulchignoni M. 1992 Huygens/ASI Plasma Wave Analyzer capabilities for aerosol measurement. In *Symposium on Titan*, ESA SP-338, pp. 229–230. ESTEC, Noordwijk, The Netherlands.

Borucki W. J., McKay C. P. and Whitten R. C. 1984 Possible production by lightning of aerosols and trace gases in Titan's atmosphere. *Icarus* **60,** 260–273.

Desch M. D. and Kaiser M. L. 1990 Upper limit set for level of lightning activity on Titan. *Nature* **343,** 442–443.

Fleagle R. G. and Businger J. A. 1963 *An Introduction to Atmospheric Physics*. Academic Press, New York.

Fulchignoni M., Angrili F., Bianchini G., Coustenis A., Grard R. J. L., Hamelin M., Liede I., McDonnell J. A. M., Neubauer F., Pellinen R., Pedersen A., Rodrigo R., Thrane E., Vanzani V., Visconti G. and Zarnecki J. C. 1990 *The Atmospheric Structure Instrument*. Proposal for the European Space Agency Huygens Probe Mission.

Grard R. 1990a A quadrupolar array for measuring the complex permittivity of the ground: application to Earth prospection and planetary exploration. *Meas. Sci. Technol.* **1,** 295–301.

Grard R. 1990b A quadrupole system for measing in situ the complex permittivity of materials: application to penetrators and landers for planetary exploration. *Meas. Sci. Technol.* **1,** 801–806.

Grard R. J. L. 1992 The significance of meteoric ionisation for the propagation of lightning spherics in the atmosphere of Titan. In *Symposium on Titan*, ESA SP-338, pp. 125–128. ESTEC, Noordwijk, The Netherlands.

Ip W.-H. 1990 Titan's upper atmosphere. *Astrophys. J.* **362,** 354–363.

Lanzerotti L. J., Thomson D. J., MacLennan C. G., Rinnert K., Krider E. P. and Uman M. A. 1989 Power spectra at radio frequency of lightning return stroke waveforms. *J. geophys. Res.* **94,** 13,221–13,227.

Lebreton J.-P. 1992 The Huygens probe. In *Symposium on Titan*, ESA SP-338. pp. 287–292. ESTEC, Noordwijk, The Netherlands.

Lellouch E. and Hunten D. M. 1987 *Titan Atmosphere Engineering Model*, ESLAB 87/199. Space Science Department of ESA/ESTEC, Noordwijk, The Netherlands.

Lindal G. F., Wood G. E., Hotz H. B. and Sweetnam D. N. 1983 The atmosphere of Titan; an analysis of the Voyager 1 radio occultation measurements. *Icarus* **53,** 348–363.

McKay C. P., Pollack J. B. and Courtin R. 1991 The greenhouse and antigreenhouse effects on Titan. *Science* **253,** 1118–1121.

Matson D. L. 1992 Cassini—a mission to Saturn and Titan, in *Symposium on Titan*, ESA SP-338, pp. 281–292. ESTEC, Noordwijk, the Netherlands.

Polk C. 1982 Schumann Resonances. In *Handbook of Atmospherics*, H. Volland (ed.), Vol. 1, pp. 111–178. CRC Press, Boca Raton, FL.

Storey L. R. O., Aubry M. P. and Meyer P. 1969 A quadrupole probe for the study of ionospheric plasma resonances. In *Plasma Waves in Space and in the Laboratory*, J. O. Thomas and B. J. Landmark (eds), Vol. 1, pp. 303–332. University Press, Edinburgh.

Uman M. A. 1987 *The Lightning Discharge*. Academic, San Diego, California.